

## Use of Arduino in the Development of a New and Fast Automated Online Preconcentration System Based on Double-Knotted Reactor for the Mn Determination in Tea Samples by Flame Atomic Absorption Spectrometry

Jeferson A. Barreto,<sup>a</sup> Valfredo A. Lemos,<sup>a</sup> Djalma M. de Oliveira,<sup>a</sup>  
Uillian Mozart F. M. Cerqueira,<sup>a</sup> Lucília A. Meira<sup>a</sup> and Marcos A. Bezerra<sup>✉</sup>\*,<sup>a</sup>

<sup>a</sup>Laboratório de Química Analítica (LQA), Universidade Estadual do Sudoeste da Bahia (UESB),  
Campus de Jequié, 45206-191 Jequié-BA, Brazil

In the present paper, an automated online preconcentration system based on the use of two knotted reactors (KR) was developed for Mn determination in tea samples by flame atomic absorption spectrometry (FAAS). The system automation was performed by using four solenoid valves to switch sample streams and reagents. Valves were driven electronically by an integrated Darlington transistor circuit and controlled by an open-source Arduino hardware platform written in C language. The preconcentration was based on the precipitation process of metal ions complexed with 2-(5-bromo-2-pyridylazo)-5-(diethylamino)phenol (5-Br-PADAP) on the inner walls of the reactor, followed by elution with a solution of hydrochloric acid. The optimized system allowed the Mn determination with limit of detection (LOD) of 2.1  $\mu\text{g L}^{-1}$ , precision (relative standard deviation (RSD), 50.0  $\mu\text{g L}^{-1}$ ) of 2.6% and enrichment factors of 8. The system presented a sampling frequency of 60  $\text{h}^{-1}$ . The method accuracy was evaluated by analysis of the certified reference material (CRM) apple leaves (NIST 1515) and by addition/recovery tests obtaining recoveries between 95.2 to 119%. This method was applied in the Mn determination in commercial tea samples purchased from local trade. Manganese levels were found in a concentration range of 2.95 to 123  $\mu\text{g g}^{-1}$ .

**Keywords:** Arduino, double-knotted reactor, automated online system, multicomutation, manganese

### Introduction

Manganese is an essential element for living beings, playing an essential role in the function of the nervous system, bone mineralization, energetic and protein metabolism, metabolic regulation and cellular protection. However, chronic exposure to this metal, especially during embryonic or postnatal stages, can induce various toxic events, in which the central nervous system is the primary target. High exposure to manganese has been associated with diseases such as Alzheimer's, amyotrophic lateral sclerosis, Parkinson's disease, schizophrenia and autism. In humans, acute and chronic effects can be generated due to exposure of high concentrations of this element, such as a dry cough, nausea, headache, fatigue, dyspnea, tremors, bronchitis, among others.<sup>1-5</sup>

Mn determination in tea samples is a timely demand because this beverage is considered healthy in the diet of humans. Their contamination by metals generally occurs as results of soil contamination by fertilizers, by industrial or mining activities, among others.<sup>6,7</sup> The European Community assesses the levels of people contamination through urine and blood analysis and evaluates the manganese concentrations levels, as usual, ranging from 0.12 to 1.9  $\mu\text{g L}^{-1}$  for urine, and 7.1 to 10.5  $\mu\text{g L}^{-1}$  for blood.<sup>8</sup> Recommended daily intakes of this element are between 1 to 5 mg through foods rich in this element, such as whole grains, legumes, nuts, almonds, fruits and teas.<sup>9</sup>

In general, analytical techniques with low-cost acquisition and maintenance such as flame atomic absorption spectrometry (FAAS) present low sensitivity in the determination of some metals in samples like tea leaves.<sup>10</sup> However, some metals present in trace levels usually require a preconcentration stage to become the determination more sensitive.<sup>10-12</sup> Knotted reactors (KR)

\*e-mail: mbezerra@uesb.edu.br

made of polytetrafluoroethylene (PTFE) have been used as a device to preconcentrate metal species with the aid of precipitating and complexing reagents, aiming to improve the sensitivity and selectivity of analytical techniques.<sup>13-15</sup> KR's have some advantages when compared to the solid-phase filled minicolumn. KR's allow high flow rates with low-pressure drops (the reactor is an open tube); they prevent loss of sensitivity due to dispersion; they are free from contamination since they are made of inert material (PTFE); KR is easy to build and inexpensive with long lifetime without efficiency losing.<sup>16,17</sup> New ideas involving the use of KR's include, as example, three-dimensional printed knotted reactors for sensitive differentiation of silver nanoparticles and ions in aqueous environmental samples,<sup>18</sup> a tandem of KR coupled with a portable tungsten coil electrothermal atomic absorption spectrometer for online determination of trace cadmium,<sup>19</sup> KR modification with activated carbon for determination of arsenic species in medicinal herbs and tea infusions,<sup>20</sup> and an association of cloud-point extraction with KR for cobalt preconcentration following by ET AAS (electrothermal AAS) determination in drinking water.<sup>21</sup>

Multicommutation is an automation strategy applied to continuous-flow analysis systems, with configurations modified by computer-controlled commutators. When the system is based on the application of solenoid valves, it is called multicommutated flow injection analysis (MCFIA). These flow systems can be easily re-configured by changing the routes of the solutions by the system using software, resulting in increased versatility, analytical speed and minimization of both reagent consumption and waste generation.<sup>22-25</sup> Multicommutation based on solenoid valves have been applied for the development of flow systems, for example, in photometric ammonium determination in rainwater,<sup>26</sup> spectrophotometric determination of reducing sugar in coconut,<sup>27</sup> salicylic acid determination in pharmaceuticals by chemiluminescent detection,<sup>28</sup> malic acid determination in wines by spectrophotometry,<sup>29</sup> among others. Total or partial automation of flow analytical methods through multicommutation systems using solenoid valves are notable devices for having several advantages such as: reducing reagent consumption, avoiding sample contamination, increasing sampling frequency, decreasing solution dispersion to the detector and decreasing of human errors.<sup>30-32</sup>

Arduino (and its clone models, such as BlackBoard, Freeduino, among others) is an electronic prototyping platform for hardware of open-source code and free software, being mounted in a single board designed with an Atmel AVR microcontroller with built-in input/output support. Arduino software uses the integrated development environment (IDE) and is available for different operating

systems. The C/C++ programming language used on Arduino boards allows creating programs for performing procedures or object-oriented. A typical Arduino board is usually composed of a controller, some digital and analog E/S lines, complementary components (that facilitate the programming and interconnection with other circuits), besides a serial or USB interface to connect to the microcomputer, which is proactively used and interact with board in real time.<sup>33-35</sup> The choice of the Arduino microprocessor was a design option and an optimization of the cost-benefit ratio. However, the circuit presented in the present article can also be developed with a PIC® microcontroller, such as those developed by ChipKIT™ or Microchip®, they are great options for FIA projects such as this presented in this study, or even more sophisticated projects. Compared with PICs, the Arduino platform is cheap and has great diversity of information, projects and forums online, facilitating the professional of Chemistry with reduced knowledge in electronics.

Methods based on the flow injection analysis for the Mn determination in food samples are still rare in the literature. In general, some extraction technique is coupled to the system for trace Mn determination in food samples using F AAS. Cloud-point extraction using 2-[2'-(6-methyl-benzothiazolylazo)]-4-bromophenol, as complexing, and Triton™ X-114, as surfactant, coupled to an FIA system was used to determine this metal with a LOD value of 0.7 µg L<sup>-1</sup> and an enrichment factor of 17.<sup>36</sup> The accuracy of the method accessed for Mn analysis was based-on certified reference material (CRM) of leaves.<sup>36</sup> In another work,<sup>37</sup> 4-(5'-bromo-2'-thiazolylazo) orcinol and the surfactant Triton X-114 were used for cloud point extraction. The LOD value, enrichment factor and sample frequency were 0.5 µg L<sup>-1</sup>, 14 and 48 h<sup>-1</sup>, respectively. Accuracy was accessed by the analysis of the certified reference biological materials rice flour and tomato leaves.<sup>37</sup> Karadaş *et al.*<sup>38</sup> have used Amberlite XAD-4 as solid-phase functionalized with 2,6-pyridinedicarboxaldehyde and its application in an online system for the preconcentration of Mn and other metals. The limit of detection (LOD) of 0.23 µg L<sup>-1</sup> and an enrichment factor of 28.9 for Mn were found.<sup>38</sup> This method was applied in the analysis of natural waters and certified reference materials such as rice flour.<sup>38</sup> Santos *et al.*<sup>39</sup> have developed an automated flow injection system based on multicommutation principle aiming to the Mn determination in vegetal leaves (chive, spinach, cauliflower, cabbage and certified reference materials of apple and spinach leaves) and natural waters. Preconcentration was carried out using an Amberlite XAD-4 minicolumn modified with 2-aminothiophenol. An improvement factor of 14 was found along with a limit of detection of 2.0 µg L<sup>-1</sup>.<sup>39</sup> Tobiasz *et al.*<sup>40</sup> have developed

a multicommuted FIA system based on solid-phase extraction (active silica gel and Dowex) for simultaneous preconcentration of manganese species. It was obtained enrichment factors of 20 and 16 and LOD values of 1.4 and 4.8  $\mu\text{g L}^{-1}$ , respectively.<sup>40</sup>

Given the great importance of developing automated analytical methods that meet society's current demands for rapid and reliable analysis of several matrices, the present work aims to use Arduino<sup>41-46</sup> in the development of an analytical approach using multivariate designs. A two-level fractionated factorial and Doehlert matrix were applied for the extraction optimization, allowing a new and rapid automated preconcentration system, using a couple of knotted reactors for the Mn determination in tea samples by F AAS.

## Experimental

### Instrumentation

The determination of metal Mn after the preconcentration steps was carried out using a PerkinElmer Analyst 200 (Waltham, Massachusetts, USA) flame atomic absorption spectrometer equipped with a deuterium lamp for background correction. Hollow cathode lamps were used following the recommendations of the manufacturer operating at the following values: 279.48 nm for wavelength, 15 mA for lamp current and 0.60 nm for bandpass for Mn determination. The flame consisted of acetylene (flow rate 2.0  $\text{L min}^{-1}$ ) and air (flow rate 13.5  $\text{L min}^{-1}$ ). The nebulizer flow rate was 5.0  $\text{mL min}^{-1}$ .

An Elga Purelab Classic (High Wycombe, UK) purification system was used to obtain ultrapure water (18.2  $\text{M}\Omega\text{ cm}$ ). The preconcentration of metals was performed in a system consisting of two multichannel peristaltic pumps from Milan (Colombo, Brazil), using silicon and PTFE tubing to propel the solutions, four solenoid valves (Cole Parmer) and handmade knotted reactor consisting of PTFE with 200 cm long, 0.5 mm internal diameter and 1.5 mm external diameter, with a 0.5 mm loop. The electronic command system consisted of an Arduino Uno R3 board with a breadboard circuit, jumpers (wires), integrated circuit ULN 2803 diode. A digester block Tecnal model 040125 (Piracicaba, Brazil) was used for the acid decomposition of the tea samples and reference certified material.

### Reagents, solutions and materials

All reagents were of analytical grade. Manganese working solutions were prepared by dilution of the

1000  $\mu\text{g mL}^{-1}$  metal stock solution (Merck, Darmstadt, Germany). Hydrochloric acid solutions were prepared by dilution of the concentrated reagent (Vetec, Duque de Caxias, Brazil) with ultrapure water. NaOH solutions were prepared from solid reagent (Vetec, Duque de Caxias, Brazil) and used to neutralize the acid digested before the buffer addition for the step of preconcentration. Acetate, phosphate and ammoniacal buffer solutions were used to keep the pH values of the standards and samples solutions submitted to preconcentration. Solutions of 2-(5-bromo-2-pyridylazo)-5-(diethylamino)-phenol (Sigma-Aldrich, Saint Louis, EUA) between 0.01 and 0.1% were prepared by dissolution of complexing reagent in anhydrous ethylic alcohol (Vetec, Duque de Caxias, Brazil).

### Sample and CRM preparation

Tea samples were purchased from a supermarket in the city of Jequié (Bahia, Brazil), taken to the laboratory, washed with deionized water, dry at 60 °C in the stove in a period of 24 h, grinding in a knife mill and passing through a sieve (300  $\mu\text{m}$ ). After this, about 0.3 g of the sample was digested by adding 10 mL of  $\text{HNO}_3$ , and 4.0 mL of  $\text{H}_2\text{O}_2$ , and all the samples were decomposed in digester block at 110 °C for 4 h. The solution's pH was adjusted with sodium hydroxide solution (1  $\text{mol L}^{-1}$ ) and borate buffer (pH 9.0). The mixture was diluted (50 mL) with deionized water. The solutions were immediately analyzed by the automatic system after preparation. Certified reference material was also digested in digester block.

### The confection of the knotted reactors

The two-knotted reactors (Figure 1) were made of PTFE polymer material, both of which were 200 cm in size, 1.5 mm in outer diameter and 0.5 mm inner diameter, and the approximate diameter of the loops was 5 mm. The PTFE tube was cut into the size to be used, interlacing it and pulling it to the ends to form a loop, avoiding a bottleneck at the nodes. This process was repeated until the complete



**Figure 1.** One of the knotted reactor used in the preconcentration system.

finalization of the reactor and its extremity connected to the automated system.

#### Automated online system programming using Arduino

In this system, an Arduino Uno R3 board used as microcontroller of the four solenoid three-way valves was used. An interface with the ULN 2803 integrated circuit was also used to make the PWM (pulse-width modulation) commands, originated in the microprocessor Arduino, switch the solenoid valves. The solenoid valves are fed by a 12 V DC and a 2.0 A current power supply. The Arduino board is powered by a 5 V DC voltage from the USB serial port of a computer (or battery), each actuated valve operates between 150 to 500 mA current. A diode was placed between the 12 V port of the integrated circuit and the 12 V supply in order to limit the voltage coming to the integrated circuit, preventing its damaging. Figure 2a shows an electrical circuit diagram of the computer board, 12 V source, Arduino, ULN 2803 integrated circuit, and the solenoid valves based on the work of Kamogawa and Miranda.<sup>35</sup> The commands used to create the control programming of the solenoid valves were written in C language for the present work, as described in Table S1 (in the Supplementary Information (SI) section). In this work, four digital ports were used, as the code written in C language in the Arduino software was recorded in the microcontroller that starts to perform the actions independently and continuously. It was not necessary to keep the microcontroller connected to the computer during the system operation.

#### Automated online system for preconcentration of Mn<sup>2+</sup>

The operation of the automated flow system (Figure 2b) can be divided into two steps for 1 min each. In step 1,

the sample with the 2-(5-bromo-2-pyridylazo)-5-diethylaminophenol (5-Br-PADAP) solution in the same line is propelled by the peristaltic pump 1 (P1), enters in the valve 2 (V2), goes to the knotted reactor 1 (KR1), the complexes Mn-5-Br-PADAP are retained on the curved inner walls of RE1 as an insoluble precipitate,<sup>47</sup> and the solution enters in the valve 3 (V3), which is also connected, and goes to a waste container (W). Meanwhile, simultaneously to this process, the peristaltic pump 2 (P2) drives the eluent passing through the valve 1 (V1), which is switched off, enters in the knotted reactor 2 (KR2), passes through the valve 4 (V4) off and goes to the waste. After the 1 min of preconcentration time at KR1 and elution at KR2, the valves are switched, the valve on, is off, and off, is on. With this in position 2, the eluent is injected into the same valves as above described (V1 and V4), now passing through KR1, extracting the analyte from the previously formed complex at position 1 and leading to FAAS detection. After 1 min again, the valves simultaneously change position, and these processes are repeated as many times as necessary (see Table 1). Thus, elution time is not considered in the calculation of the sampling frequency because of the change of position alternately in the preconcentration stage for both processes, P2 is switched off after the measurement in the FAAS, being switched for elution. Absorbance signals obtained by this system were registered as a transient signal.

#### Multivariate optimization of the automated flow system

Multivariate designs were used to optimize the flow preconcentration system based on a double-knotted reactor. Two level fractional factorial design  $2^{5-1}$  was used for the screening of the variable<sup>48</sup> concentration of HCl as eluent, the concentration of 5-Br-PADAP complexing reagent, sample flow, pH and buffer concentration, which can

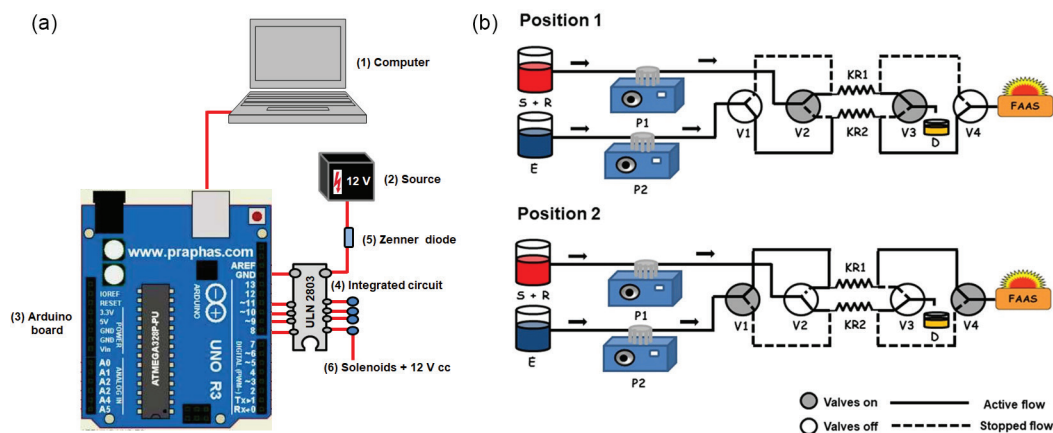


**Figure 2.** (a) Schematic diagram of the electrical part involving (1) computer, (2) source, (3) Arduino, (4) integrated circuit, (5) Zener diode and (6) solenoid valves; (b) steps of the automated online preconcentration system for Mn determination using double-knotted reactor.

**Table 1.** Automatic solenoid valve operation of the 2-step cyclic preconcentration and Mn determination by knotted reactor coupled to flow injection analysis-flame atomic absorption spectrometry

Step	time / s	Flow pathway	Solenoid valve state			
			V1	V2	V3	V4
1	60	P1: [sample + 5-Br-PADAP sol.] → V2 → KR1: [Mn(5-Br-PADAP)n] (preconc.) → V3 → waste P2: [eluent] → V1 → KR2 → V4 → F AAS detector	off	on	on	off
2	60	P1: [sample + 5-Br-PADAP sol.] → V2 → KR2: [Mn(5-Br-PADAP)n] (preconc.) → waste P2: [eluent] → V1 → KR1 → V4 → F AAS detector	on	off	off	on

P1 and P2: pump 1 and pump 2; V1 to V4: solenoid valves; KR1 and KR2: knotted reactors; precon.: metal preconcentration by complexation with 2-(5-bromo-2-pyridylazo)-5-diethylaminophenol; F AAS: flame atomic absorption spectrometry.

significantly affect the performance of the preconcentration system. The Doehlert design<sup>49</sup> was applied to find the optimal points of the variables considered significant. The experimental data were processed in Statistica 10 software<sup>50</sup> at a 95% confidence level. The online preconcentration system was based on the time of 1 min. In the optimization step, solutions of 50 µg L<sup>-1</sup> Mn<sup>2+</sup> were used, and the absorbance was used as the analytical response. All experiments were carried out in aleatory order.

## Results and Discussion

### Optimization of the automated system

Fractional factorial design 2<sup>5-1</sup> was applied to investigate the influence of five variables on the automated preconcentration system. The evaluated variables were the

sample flow rate (SFR), pH, buffer concentration (BC), complexing reagent concentration (CCR) and eluent concentration (EC). The studied variables, their high and low levels, the experimental matrix and the responses (in absorbance) are presented in Table 2. The main effects of the variables were evaluated adopting a confidence level of 95%. Pareto graph is a bar chart that illustrates the magnitude of the effects and allows easy visualization of the significance of the variables. Pareto graph shown in Figure 3 indicates that the variable, that most influences the magnitude of the response, is the sampling flow rate (SFR). This signal increase occurs due to the fact that the preconcentration system is based on time. An increase in the sampling flow rate tends to carry a significant amount of analyte mass to be concentrated in the knotted reactor. The second most significant variable was pH. Basic pH favors the formation reaction of the insoluble complex, precipitating and retaining it in the curves of the

**Table 2.** Experimental matrix and response as Mn absorbance for the two-level fractional factorial design 2<sup>5-1</sup>

Experiment	SFR / (mL min <sup>-1</sup> )	CRC (m v <sup>-1</sup> ) / %	pH	BC / (mol L <sup>-1</sup> )	EC / (mol L <sup>-1</sup> )	Absorbance
1	10.0 (+1)	0.1 (+1)	9.0 (+1)	0.5 (+1)	1.0 (+1)	0.023 / 0.022
2	10.0 (+1)	0.1 (+1)	9.0 (+1)	0.1 (-1)	0.1 (-1)	0.033 / 0.026
3	10.0 (+1)	0.1 (+1)	7.0 (-1)	0.5 (+1)	0.1 (-1)	0.035 / 0.031
4	10.0 (+1)	0.1 (+1)	7.0 (-1)	0.1 (-1)	1.0 (+1)	0.043 / 0.048
5	10.0 (+1)	0.01 (-1)	9.0 (+1)	0.5 (+1)	0.1 (-1)	0.048 / 0.054
6	10.0 (+1)	0.01 (-1)	9.0 (+1)	0.1 (-1)	1.0 (+1)	0.063 / 0.071
7	10.0 (+1)	0.01 (-1)	7.0 (-1)	0.5 (+1)	1.0 (+1)	0.023 / 0.021
8	10.0 (+1)	0.01 (-1)	7.0 (-1)	0.1 (-1)	0.1 (-1)	0.017 / 0.018
9	5.0 (-1)	0.1 (+1)	9.0 (+1)	0.5 (+1)	0.1 (-1)	0.016 / 0.011
10	5.0 (-1)	0.1 (+1)	9.0 (+1)	0.1 (-1)	1.0 (+1)	0.010 / 0.011
11	5.0 (-1)	0.1 (+1)	7.0 (-1)	0.5 (+1)	1.0 (+1)	0.011 / 0.014
12	5.0 (-1)	0.1 (+1)	7.0 (-1)	0.1 (-1)	0.1 (-1)	0.018 / 0.020
13	5.0 (-1)	0.01 (-1)	9.0 (+1)	0.5 (+1)	1.0 (+1)	0.015 / 0.014
14	5.0 (-1)	0.01 (-1)	9.0 (+1)	0.1 (-1)	0.1 (-1)	0.026 / 0.023
15	5.0 (-1)	0.01 (-1)	7.0 (-1)	0.5 (+1)	0.1 (-1)	0.015 / 0.010
16	5.0 (-1)	0.01 (-1)	7.0 (-1)	0.1 (-1)	1.0 (+1)	0.014 / 0.010

SFR: sampling flow rate; CRC: complexing reagent concentration; BC: buffer concentration; EC: eluent concentration; coded values are in brackets.

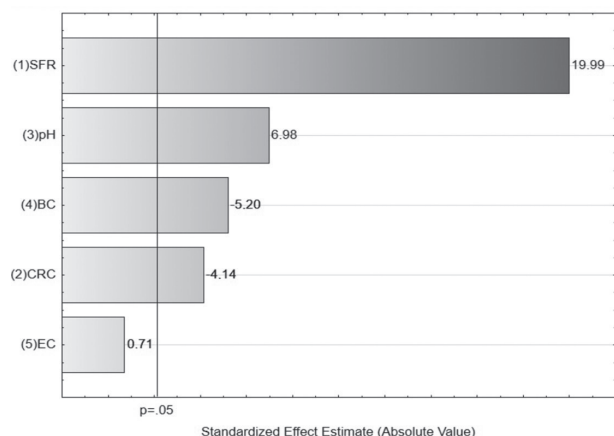


**Figure 3.** Pareto graph for the variables studied using fractional factorial design  $2^{5-1}$  in the Mn preconcentration system.

reactor. In this way, the more precipitous the formation, higher the signal is.

The compound 5-Br-PADAP behave as an *N,N,O*-terdentate ligand to form  $\text{Mn}(5\text{-Br-PADAP})_2$  or its  $\text{ML}_2$  chelate. The optimum pH range for this complexation depends on the  $\text{Mn}(\text{OH})_2$  solubility product ( $K_{\text{ps}} = 1.9 \times 10^{-9}$  at  $25^\circ\text{C}$ ) and th is e concentration of 5-Br-PADAP ionized form ( $\text{p}K_{\text{a}1} = 0.1$ ,  $\text{p}K_{\text{a}2} = 2.0$  and  $\text{p}K_{\text{a}3} = 11.3$ ). The operational pH is kept below 9.0 to prevent the formation of metal hydroxides, which precipitates before the introduction of the sample solution in the system.<sup>51</sup>

On the other hand, the variables buffer concentration (BC) and complexing reagent concentration (CRC) presented significant effects and negative values, indicating that working on the lower levels of these two variables, contributes to increase the Mn extraction by the knotted reactor. The complexing reagent is diluted in an alcoholic solution, and several volumes of this solution are used to increase the complexing reagent concentration in

the final solution of the sample submitted to the online preconcentration system. The higher the ethyl alcohol concentration in the final solution, the higher the solubility of the Mn-Br-PADAP complex and the lower the analytical signal obtained. Eluent concentration (EC) does not present a significant effect in the studied experimental interval, and its value was kept to a low level ( $0.1 \text{ mol L}^{-1}$ ).

In a second optimization step, Doehlert design was applied to better model the data set and to locate the optimum values with more accuracy for the extraction of the Mn using the automated system based on the double-knotted reactor. The three more significant variables (SFR, pH and BC) were selected for this step. Complexing reagent concentration was kept at its low level ( $0.01\% \text{ m v}^{-1}$ ). The obtained experimental matrix and the responses are presented in Table 3.

Mathematical models (linear and quadratic) were fitted to the responses obtained from the application of the Doehlert matrix in order to describe the behavior of the experimental data and to make statistically valid predictions about the location of the optimal values of the studied variables. Both the linear and the quadratic models showed a significant lack-of-fit (calculated  $F >$  tabled  $F$ ), as showed in Table 4. However, the quadratic model presents smaller residuals and higher correlation coefficient ( $R = 0.8901$ ) between the predicted values and the observed values with the linear model ( $R = 0.7502$ ), as shown in Figure 4. Thus, the quadratic model was chosen to model the data.<sup>52</sup>

The equation obtained by the fitting of the quadratic function, composed only by the significant terms, is presented below:

$$\text{Abs} = (0.189 \pm 0.056) + (0.0020 \pm 0.00045) \text{SRF}^2 - (0.0564 \pm 0.0076) \text{pH} + (0.00650 \pm 0.00045) \text{pH}^2 - (0.00300 \pm 0.00052) \text{SRF} \times \text{pH} \quad (1)$$

**Table 3.** Doehlert matrix applied to optimization of the automated preconcentration system based on the knotted reactor

Experiment	SRF / ( $\text{mL min}^{-1}$ )	pH	BC / ( $\text{mol L}^{-1}$ )	Absorbance
1	8 (0)	9 (1)	0.2 (0)	0.066 / 0.060
2	7 (-0.5)	8 (0.5)	0.1 (-0.866)	0.016 / 0.016
3	7 (-0.5)	8 (0.5)	0.3 (0.866)	0.016 / 0.012
4	9 (0.5)	8 (0.5)	0.1 (-0.866)	0.020 / 0.021
5	9 (0.5)	8 (0.5)	0.3 (0.866)	0.022 / 0.020
6	6 (-1)	7 (0)	0.2 (0)	0.012 / 0.014
7	8 (0)	7 (0)	0.2 (0)	0.008 / 0.003
8	10 (1)	7 (0)	0.2 (0)	0.014 / 0.014
9	7 (-0.5)	6 (-0.5)	0.1 (-0.866)	0.000 / 0.000
10	7 (-0.5)	6 (-0.5)	0.3 (0.866)	0.000 / 0.000
11	9 (0.5)	6 (-0.5)	0.1 (-0.866)	0.016 / 0.019
12	9 (0.5)	6 (-0.5)	0.3 (0.866)	0.020 / 0.016
13	8 (0)	5 (-1)	0.2 (0)	0.000 / 0.000

SRF: sampling flow rate; BC: buffer concentration; coded values are in brackets.

Two partial response surfaces related to the quadratic model are shown in Figure 5. These considerations are only valid within the studied experimental field, and

extrapolations out of the smaller adopted values for these variables cannot be performed because the empirical model fitted to the data is local.

**Table 4.** Analysis of variance for the linear and quadratic model fitted to data from Table 3

Linear model					
Variation source	SS	df	MS	Calculated $F$	Tabled $F$
Regression	0.003580	3	0.001193	9.44	3.05
Residuals	0.002782	22	0.000126		
Lack-of-fit	0.002726	9	0.000303	70.9	2.71
Pure error	0.000056	13	0.000004		
Total SS	0.006362	25			
Quadratic model					
Variation source	SS	df	MS	Calculated $F$	Tabled $F$
Regression	0.005039	9	0.000560	6.77	2.54
Residuals	0.001323	16	0.000083		
Lack-of-fit	0.001267	3	0.000422	98.9	3.41
Pure error	0.000056	13	0.000004		
Total SS	0.006362	25			

SS: sum of the square; df: degree of freedom; MS: medium of square.

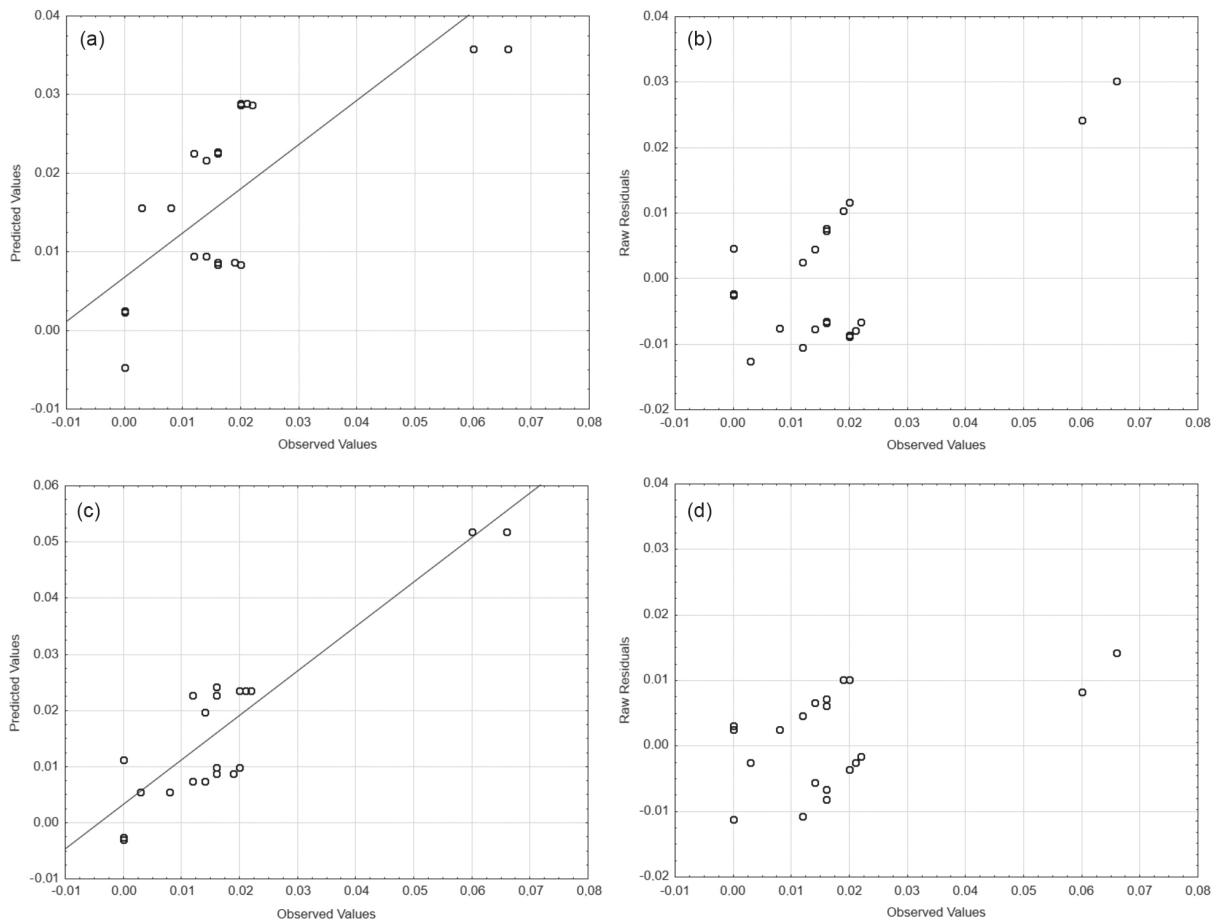


**Figure 4.** Evaluation of linear (a and b) and quadratic (c and d) models fitted to experimental data obtained from Doehlert design; observed vs. predicted values graphs (a and c) and residual graphs (b and d).

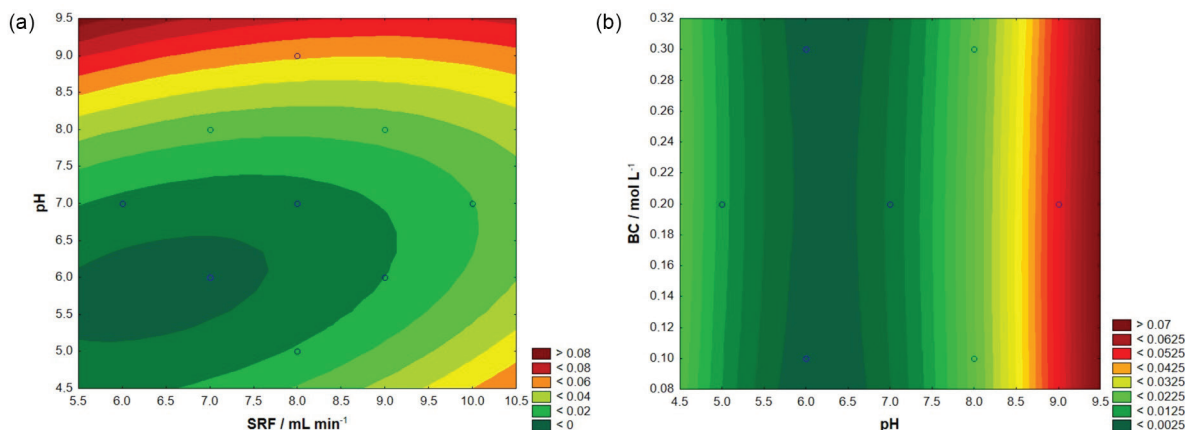


**Figure 5.** Two partial level curve obtained after Doehlert design application: (a) pH  $\times$  sample flow rate (SFR) and (b) pH  $\times$  buffer concentration (BC) in the Mn determination.

Analysis of the level curves reveals that the highest responses are obtained when the preconcentration is performed at a sampling flow rate of 10.0 mL min<sup>-1</sup> at pH 9.0 and buffer concentration of 0.3 mol L<sup>-1</sup>.

#### Study of the preconcentration time

The study of preconcentration time in the online automated systems is an essential factor because it is directly related to the sampling frequency. The preconcentration time was varied in the range of 0.5 to 3.0 min, and the results are shown in Figure 6. This figure reveals an increase in the signals for the Mn from 0.5 to 1.0 min. Between 1.0 and 3.0 min, it is observed that the signal remains constant. This behavior is due to saturation of the knotted reactor, i.e., the capacity of the reactor to retain Mn<sup>2+</sup> as precipitated complexes reaches its maximum. In order to maintain an excellent analytical frequency and the low consumption index of the sample with good sensitivity, the time of 1.0 min was chosen.

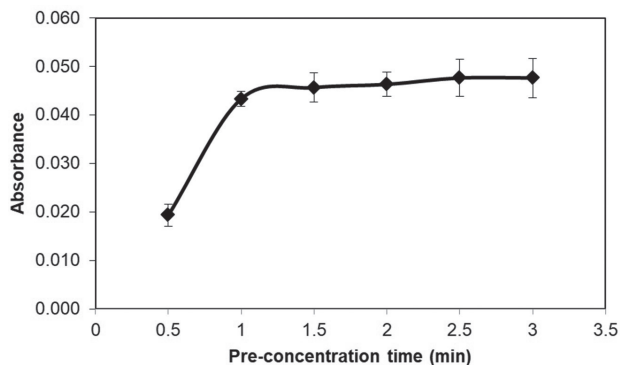


**Figure 6.** Study of preconcentration time for Mn determination using the automated system based on double-knotted reactor working in the optimum conditions.

#### Analytical characteristics

The analytical characteristics were established using the optimum conditions found in the multivariate optimization process of the automated preconcentration system for Mn determination.

Analytical curves were obtained by subjecting the standard solutions to the preconcentration system. Solutions between concentrations of 2.00 to 100.0  $\mu\text{g L}^{-1}$  provided the following curve:

$$A = 6.31 \times 10^{-4} C_{\text{Mn}} (\mu\text{g L}^{-1}) + 1.88 \times 10^{-3} \quad (R^2 = 0.9991) \quad (2)$$

For the direct reading (curve without preconcentration of the standard solutions), the curve obtained was

$$A = 8.0 \times 10^{-5} C_{\text{Mn}} (\mu\text{g L}^{-1}) - 0.0006 \quad (R^2 = 0.9997) \quad (3)$$

for Mn solutions with concentrations between 500 and 2000  $\mu\text{g L}^{-1}$ .

The enrichment factor was calculated by: (i) the ratio between the angular coefficients of the curve where there were the preconcentration and the curve found by direct determination (without preconcentration) of the Mn standards, and (ii) comparing the digested sample signal with and without the preconcentration. The enrichment factors found by these methodologies were between 8 to 9.5 times.

LOD and LOQ (limit of quantification) were found according to the following definition:  $\text{LOD} = 3s / S$  and  $\text{LOQ} = 10s / S$ , where  $s$  is the standard deviation of twelve consecutive measurements of the blank signal and  $S$  is the slope of analytical curve. Values found for LOD and LOQ were 0.070 and 0.23  $\mu\text{g g}^{-1}$ , respectively. Precision was accessed as repeatability (relative standard deviation (RSD) in %,  $n = 10$ ), and it was found values such as 2.6%

(50  $\mu\text{g L}^{-1}$ ) and 3.2% (100  $\mu\text{g L}^{-1}$ ). Parameters of efficiency from automated preconcentration system were also accessed. The system presented an analytical frequency of 60  $\text{h}^{-1}$ , concentration efficiency of 8  $\text{min}^{-1}$  and consumption index of 1.25 mL.

Accuracy was evaluated by the analysis of the certified reference material apple leaves NIST 1515 and addition/recovery tests. The result found by the analysis of the certified material using the automated system was  $52.0 \pm 5.0 \mu\text{g g}^{-1}$ . The certified value is  $54.0 \pm 3.0 \mu\text{g g}^{-1}$ , and the *t*-test showed that the result did not show a significant difference with the certified value using a confidence level of 95%. Table 5 shows the results obtained for two samples in the addition/recovery tests. Recoveries of 95.2 and 105% were found for the two samples, being considered satisfactory to take into account the trace levels of the analyte.

**Table 5.** Addition and recovery assays of Mn in tea leaves using the proposed method, with the 95% confidence interval ( $n = 3$ )

Tea sample	Mn concentration		Recovery / %
	Added / ( $\mu\text{g g}^{-1}$ )	Found / ( $\mu\text{g g}^{-1}$ )	
Lemongrass	0	3.0	95.2
	4.2	7.0	
Pitanga	0	< LOQ	105
	4.2	4.4	

LOQ: limit of quantification.

Mn determination in tea samples using the developed method

After verifying that the developed system has analytical characteristics for the Mn determination in the tea samples, six samples of industrialized tea commercialized in the city of Jequié (Bahia, Brazil) were analyzed. The results are shown in Table 6.

**Table 6.** Mn determination from commercial tea samples using the proposed automated preconcentration system based on double-knotted reactor proposed

Tea sample	Concentration <sup>a</sup> / ( $\mu\text{g g}^{-1}$ )
Mint	$3.0 \pm 0.8$
Mate	$123 \pm 18$
Green	$108 \pm 2$
Black	$119 \pm 5$
Citric	$18.8 \pm 0.6$
Strawberry	$8.8 \pm 0.8$

<sup>a</sup>Average  $\pm$  standard deviation ( $n = 3$ ).

## Conclusions

The developed preconcentration system, using a double-knotted reactor, has presented adequate analytical characteristics in the Mn determination in samples of tea leaves. The automation of the preconcentration system using solenoid valves, controlled by an integrated circuit interconnected to an Arduino board, allowed to obtain an excellent precision, with the reduction of operational errors. The configuration of the automated online system with the double-knotted reactors was proposed for the first time in this work, seeking a more straightforward format possible without loss of efficiency. The method was applied in the Mn determination in samples of commercial tea leaves purchased in the local market of the city of Jequié (Bahia, Brazil). Manganese contents found in these samples were between 2.95 and 122.89  $\mu\text{g g}^{-1}$  for the analyzed samples.

## Supplementary Information

Supplementary data are available free of charge at <http://jbs.sbq.org.br> as PDF file.

## Acknowledgments

The authors acknowledge grants and fellowships from the Conselho Nacional de Desenvolvimento Científico e Tecnológico (CNPq), Fundação de Amparo à Pesquisa do Estado da Bahia (FAPESB) and Coordenação de aperfeiçoamento de Pessoal de Nível Superior (Capes).

## References

1. Michalke, B.; Fernsebner, K.; *J. Trace Elem. Med. Biol.* **2014**, *28*, 106.
2. Lucchini, R. G.; Martin, C. J.; Doney, B. C.; *Neuromol. Med.* **2009**, *11*, 311.
3. Aschner, M.; Erikson, K. M.; Hernandez, E. H.; Tjalkens, R.; *Neuromol. Med.* **2009**, *11*, 252.
4. Azevedo, F. A.; Chasin, A. A. M.; *Metals: Gerenciamento da Toxicidade*, 1<sup>a</sup> ed.; Atheneu, São Paulo, Brasil, 2003.
5. Michalke, B.; Halbach, S.; Nischwitz, V.; *J. Environ. Monit.* **2007**, *9*, 650.
6. Oliveira, L. M.; Das, S.; Silva, E. B.; Gao, P.; Gress, J.; Liu, Y.; Ma, L. Q.; *Sci. Total Environ.* **2018**, *633*, 649.
7. Han, W. Y.; Shi, Y. Z.; Ma, L. F.; Ruan, J. Y.; *Bull. Environ. Contam. Toxicol.* **2005**, *75*, 272.
8. Neves, E. B.; Mendonça Jr., N.; Moreira, M. F. R.; *Cienc. Saúde Colet.* **2009**, *4*, 2269.

9. Martins, I.; Lima, I. V.; *Ecotoxicologia do Manganês e seus Compostos*, vol. 1 - *Série Cadernos de Referência Ambiental no. 7*; CRA: Salvador, Brasil, 2001.
10. Ferreira, S. L. C.; Bezerra, M. A.; Santos, A. S.; Santos, W. N. L.; Novaes, C. G.; Oliveira, O. M. C.; Oliveira, M. L.; Garcia, R. L.; *TrAC, Trends Anal. Chem.* **2018**, *100*, 1.
11. Xiong, C.; Chen, X.; Liu, X.; *Chem. Eng. J.* **2012**, *203*, 115.
12. Chen, S.; Li, J.; Lu, D.; Zhang, Y.; *Food Chem.* **2016**, *211*, 741.
13. Souza, A. S.; Santos, W. N. L.; Ferreira, S. L. C.; *Spectrochim. Acta, Part B* **2005**, *60*, 737.
14. Cerutti, S.; Martinez, L. D.; Wuilloud, R. G.; *Appl. Spectrosc. Rev.* **2005**, *40*, 71.
15. Dimitrova, B.; Benkhedda, K.; Ivanova, E.; Adams, F.; *J. Anal. At. Spectrom.* **2004**, *19*, 1394.
16. Fernández, O. R.; Wuilloud, R. G.; Wuilloud, J. C.; Olsina, R. A.; Martinez, L. D.; *J. AOAC Int.* **2002**, *85*, 1410.
17. Salonia, J. A.; Gasquez, J. A.; Martinez, L. D.; Cerutti, S.; Kaplan, M.; Olsina, R. A.; *Instrum. Sci. Technol.* **2006**, *34*, 305.
18. Su, C.; Hsieh, M.; Sun, Y.; *Anal. Chim. Acta* **2016**, *914*, 110.
19. Wen, X.; Yang, S.; Zhang, H.; Deng, Q.; *Microchem. J.* **2016**, *124*, 60.
20. Grijalba, A. C.; Martinis, E. M.; Lascalea, G. E.; Wuilloud, R. G.; *Spectrochim. Acta, Part B* **2015**, *103*, 49.
21. Gil, R. A.; Gásquez, J. A.; Olsina, R.; Martinez, L. D.; Cerutti, S.; *Talanta* **2008**, *76*, 669.
22. Llorent-Martinez, E.; Barrales, P.; Fernandez de Cordova, M.; Ruiz-Medina, A.; *Curr. Pharm. Anal.* **2010**, *6*, 53.
23. Leal, L. O.; Ferrer, L.; Forteza, R.; Cerdà, V.; *TrAC, Trends Anal. Chem.* **2011**, *30*, 761.
24. Feres, M. A.; Zagato, E. A. G.; Santos, J. L. M.; Lima, J. L. F. C. In *The Concept of Multi-Commutation in Flow Analysis in Advances in Flow Analysis*; Trojanowicz, M., ed.; Wiley: New Jersey, USA, 2008.
25. Rocha, F. R. P.; Reis, B. F.; Zagatto, E. A. G.; Lima, J. L. F. C.; Lapa, R. A. S.; Santos, J. L. M.; *Anal. Chim. Acta* **2002**, *468*, 119.
26. Vieira, G. P.; Crispino, C. C.; Perdigo, S. R. W.; Reis, B. F.; *Anal. Methods* **2012**, *5*, 489.
27. Silva, A. B.; Souza, G. C. S.; Alves, A. A.; Belian, M. F.; Galembeck, A.; Lavorante, A. F.; *Food Control* **2015**, *57*, 225.
28. Llorent-Martínez, E. J.; Ortega-Barrales, P.; Molina-Díaz, A.; *Anal. Chim. Acta* **2006**, *580*, 149.
29. de Santana, J. F. S.; Belian, M. F.; Lavorante, A. F.; *Anal. Sci.* **2014**, *30*, 657.
30. Cerdà, A.; Cerdà, V.; *An Introduction to Flow Analysis*, 1<sup>st</sup> ed.; Sciware: Palma de Mallorca, Spain, 2009.
31. Clavijo, S.; Avivar, J.; Suárez, R.; Cerdà, V.; *TrAC, Trends Anal. Chem.* **2015**, *67*, 26.
32. Lemos, V. A.; Bezerra, M. A.; *Análises Químicas por Sistemas de Injeção em Fluxo*; Edições UESB: Vitória da Conquista, Brasil, 2017.
33. Arduino software, available at <https://www.arduino.cc/en/Main/Software>, 2018, accessed in May 2019.
34. Rosa, T. R.; Betim, F. S.; Ferreira, R. Q.; *Electrochim. Acta* **2017**, *231*, 185.
35. Kamogawa, M. Y.; Miranda, J. C.; *Quim. Nova* **2013**, *36*, 1232.
36. Lemos, V. A.; David, G. T.; *Microchem. J.* **2010**, *94*, 42.
37. Lemos, V. A.; Baliza, P. X.; Carvalho, A. L.; Oliveira, R. V.; Teixeira, L. S. G.; Bezerra, M. A.; *Talanta* **2008**, *77*, 388.
38. Karadaş, C.; Turhan, O.; Kara, D.; *Food Chem.* **2013**, *141*, 655.
39. Santos, Q. O.; Novaes, C. G.; Bezerra, M. A.; Lemos, V. A.; Moreno, I.; Silva, D. G.; Santos, L.; *J. Braz. Chem. Soc.* **2010**, *21*, 2340.
40. Tobiasz, A.; Sołtys, M.; Kurys, E.; Domagała, K.; Walas, S.; *Spectrochim. Acta, Part B* **2017**, *134*, 11.
41. Pearce, J. M.; *Science* **2012**, *337*, 1303.
42. Grinias, J. P.; Whitfield, J. T.; Guetschow, E. D.; Kennedy, R. T.; *J. Chem. Educ.* **2016**, *93*, 1316.
43. Rosa, T. R.; Betim, F. S.; Ferreira, R. Q.; *Electrochim. Acta* **2017**, *231*, 185.
44. Ng, S. M.; Wong, D. S.; Phung, J. H.; Chua, H. S.; *Talanta* **2013**, *116*, 514.
45. González, P.; Pérez, N.; Knochen, M.; *Quim. Nova* **2016**, *39*, 305.
46. Urban, P. L.; *Analyst* **2015**, *140*, 963.
47. Wen, X.; Wu, P.; Xu, K.; Wang, J.; Hou, X.; *Microchem. J.* **2009**, *91*, 193.
48. Neto, B. B.; Scarmínio, I. S.; Bruns, R. E.; *Como Fazer Experimentos*, 4<sup>th</sup> ed.; Bookman: Porto Alegre, Brasil, 2010.
49. Ferreira, S. L. C.; Santos, W. N. L.; Quintella, C. M.; Neto, B. B.; Bosque-Sendra J. M.; *Talanta* **2004**, *63*, 1061.
50. *Statistica Software 10.0*; StatSoft, Tulsa, OK, USA, 2010.
51. Ueno, K.; Imamura, T.; Cheng, K. L.; *Handbook of Organic Analytical Reagents*; CRC Press: Boca Raton, USA, 1992.
52. Bezerra, M. A.; Santelli, R. E.; Oliveira, E. P.; Villar, L. S.; Escaleira, L. A.; *Talanta* **2008**, *76*, 965.

Submitted: October 22, 2018

Published online: May 28, 2019

